Supplement of Clim. Past Discuss., 11, 637–670, 2015
http://www.clim-past-discuss.net/11/637/2015/
doi:10.5194/cpd-11-637-2015-supplement

Climate of the Past Discussions
Open Access

Supplement of

Trace metal evidence for a poorly ventilated glacial Southern Ocean

M. Wagner and I. L. Hendy

Correspondence to: M. Wagner (wagne2me@cmich.edu)

Supplement

S1. ^{230}Th Normalization

Lateral sediment redistribution is a well-documented phenomenon in the Southern Ocean that can deposit up to 20 times more sediment than the vertical rain at a given site (Chase et al., 2003; Dezileau et al., 2000; Francois et al., 1993). To correct for this, prior studies have normalized proxy concentrations to ^{230}Th (e.g., Anderson et al., 2009; Bradtmiller et al., 2009; Chase et al., 2003), which also generates fluxes of proxies to the sediment-water interface (Francois et al., 2004). Thorium-230 has a known production rate in the water column, and its expected flux to sediments is entirely a function of water depth. Preserved vertical fluxes of sedimentary components are calculated from measured excess ^{230}Th and normalized to the expected flux of ^{230}Th to sediments (Francois et al., 2004):

$$F_i = (\beta \times z \times f_i)/_{xs}{}^{230}\mathrm{Th}_0 \quad (1)$$

where F_i is the preserved vertical flux of component i; β is the production rate of ^{230}Th in the water column (2.63×10^{-5} dpm/cm^3/kyr); z is water depth in cm; f_i is the weight fraction of component i; and $_{xs}{}^{230}\mathrm{Th}_0$ is the measured sedimentary ^{230}Th not associated with the detrital component.

S2. Trace Metal Fluxes

To assess whether interpretation of redox chemistry may have been affected by sediment redistribution, trace metal and organic carbon concentrations (Tables S1-S4) were normalized to ^{230}Th. Published $_{xs}{}^{230}\mathrm{Th}_0$ data (Anderson et al., 2009, archived data; Kumar et al., 1995, Table S5) and modern water depths for cores were used to calculate preserved vertical fluxes to sediments. $_{xs}{}^{230}\mathrm{Th}_0$ values were linearly interpolated between data points, except for sampled intervals at the tops of the cores above the first data point, which were assigned the same $_{xs}{}^{230}\mathrm{Th}_0$

value as the first data point; and sampled intervals below the last data point (884 cm) in TN057-13-4PC, which were assigned the same $_{xs}^{230}Th_0$ value as the last data point. Errors for interpolated $_{xs}^{230}Th_0$ values were estimated by calculating one standard deviation of the $_{xs}^{230}Th_0$ values immediately above and below the sampled interval. Errors in $_{xs}^{230}Th_0$ and trace metal concentrations were propagated at the 1σ level when calculating trace metal fluxes.

Given that trace metals precipitate at a redox front within sediments, and ^{230}Th is delivered to the sediment-water interface in association with particles, a vertical offset between trace metals and ^{230}Th can occur. However, this offset is likely minimal (see Section 2.1) and less important given large other uncertainties present in calculating trace metal fluxes (discussed below).

Total uncertainty in trace metal fluxes arises mostly from low data density for $_{xs}^{230}Th_0$ values in RC13-254, and the choice to linearly interpolate between data points for both cores. Without additional data points, the true variation in RC13-254 $_{xs}^{230}Th_0$ values is unknown. In comparison, uncertainties in trace metal fluxes for TN057-13-4PC are much smaller and of less concern, particularly during deglaciation, and they will not be considered further. For RC13-254, large uncertainties in trace metal fluxes make it largely impossible to discern variation through time, with the exception of ~140 cm (~17.7 ka). However, we can consider two extreme cases: that the true trace metal fluxes are either at the upper or lower bounds of the uncertainty window. If fluxes are at the upper bound, this strongly indicates reducing conditions in sedimentary pore waters from high export productivity and/or low bottom water oxygen prior to ~13.5 ka (below ~65 cm core depth). If fluxes are at the lower bound, there is a smaller—but discernible—difference between the intervals of ~3.5-15.6 ka (0-102 cm; burndown interval) and ~15.6-29 ka (102-380 cm) [Figure S1], indicating a change to better oxygenated conditions sometime after

~15.6 ka. Trace metal fluxes (Figures S1 and S2) are, however, consistent with total bulk sediment trace metal concentrations (Figures 3 and 4) in that they demonstrate higher input to sediments during the last glacial period and deglaciation. Furthermore, correspondence with $\Delta^{14}C$ ventilation records (Skinner et al., 2010; see Section 4.3; Skinner et al., 2014) and organic carbon concentrations/fluxes (Figures 3 and 4; Figures S1 and S2) argues against trace metal accumulation being an artifact of sediment focusing.

One important difference between trace metal fluxes and concentrations arises at site TN057-13-4PC from ~17 ka (~770 cm) onward. Normalization to ^{230}Th produces several peaks in Ag and Re fluxes that do not otherwise appear or are muted when plotting total bulk sediment trace metal concentrations. Elevated opal (Figure 4f) and organic carbon (Figure S2) fluxes suggest that any trace metal enrichments are productivity driven.

Supplementary Figure Captions

Figure S1. Trace metal and organic carbon fluxes for RC13-254.

Figure S2. Trace metal and organic carbon fluxes for TN057-13-4PC.

Supplementary Tables

Table S1. TN057-13-4PC trace metal concentrations.

Depth (cm)	Age (yr)	Cd (ppm)	± 1σ (ppm)	Re (ppb)	± 1σ (ppb)	Ag (ppb)	± 1σ (ppb)	Mo (ppm)	± 1σ (ppm)
0-1	18	0.06	0.01	0.5	0.0	69	15	0.46	0.10
10-11	305	0.10	0.02	0.4	0.0	19	3	1.29	0.22
20-21	749	0.03	0.01	0.4	0.0	45	6	0.18	0.00
40-41	1259	0.07	0.01	0.4	0.0	37	5	0.12	0.00
60-61	1769	0.08	0.02	0.5	0.0	70	10	0.08	0.00
80-81	2295	0.10	0.02	0.7	0.0	79	11	0.08	0.00
100-101	2824	0.10	0.02	0.6	0.0	74	10	0.14	0.00
120-121	3353	0.10	0.02	0.6	0.0	61	9	0.18	0.04
140-141	3882	0.12	0.02	1.0	0.0	71	10	0.10	0.00
160-161	4410	0.13	0.02	0.6	0.0	38	8	0.12	0.00
180-181	4939	0.14	0.03	1.0	0.0	63	9	0.12	0.00
200-201	5468	0.20	0.04	1.0	0.0	81	11	0.12	0.00
220-221	5997	0.26	0.05	2.4	0.1	142	20	0.16	0.00
240-241	6526	0.25	0.04	13.3	0.6	145	31	0.47	0.08
260-261	6998	0.24	0.04	9.9	0.5	87	12	0.45	0.01
300-301	7549	0.19	0.03	4.1	0.2	88	12	0.48	0.01
340-341	8100	0.20	0.04	3.6	0.2	125	18	0.53	0.01
380-381	8651	0.18	0.07	4.4	0.2	148	32	0.52	0.01
420-421	9203	0.17	0.03	1.9	0.1	74	10	0.39	0.01
470-471	9631	0.11	0.02	2.1	0.1	82	11	0.33	0.05
510-511	10164	0.10	0.02	2.7	0.1	84	18	0.39	0.01
560-561	10988	0.10	0.02	1.6	0.1	94	13	0.22	0.03
580-581	11367	0.09	0.02	0.8	0.0	76	11	0.30	0.00
610-611	11936	0.09	0.02	1.0	0.0	40	9	0.27	0.00
640-641	12505	0.08	0.02	1.5	0.1	45	6	0.26	0.00
670-671	13073	0.14	0.03	1.2	0.1	82	11	0.31	0.00
700-701	13642	0.15	0.03	2.7	0.1	81	11	0.71	0.01
730-731	14211	0.16	0.03	4.2	0.2	95	13	0.79	0.01
760-761	16163	0.13	0.02	9.6	0.5	93	13	0.86	0.14
770-771	17062	0.26	0.14	4.6	0.2	87	19	1.17	0.02
780-781	17960	0.34	0.06	5.0	0.2	130	18	1.31	0.23
790-791	18859	0.43	0.08	6.4	0.3	200	28	1.25	0.02
800-801	19758	0.42	0.07	13.0	0.6	216	47	1.38	0.23
810-811	20657	0.32	0.06	7.3	0.3	218	31	1.28	0.02
820-821	21556	0.23	0.04	3.7	0.2	71	15	1.03	0.18
830-831	22454	1.13	0.20	7.4	0.4	382	53	0.62	0.11

840-841	23353	1.13	0.20	9.0	0.4	589	82	0.75	0.01
850-851	24252	1.24	0.22	14.2	0.7	366	81	0.84	0.14
860-861	25151	0.99	0.18	11.8	0.5	267	37	0.78	0.01
870-871	26050	0.78	0.14	15.3	0.7	154	22	0.99	0.17
880-881	26949	0.73	0.13	26.4	1.2	114	16	0.86	0.01
890-891	27847	0.69	0.12	64.8	3.1	119	17	1.39	0.23
900-901	28746	0.60	0.11	41.2	2.0	98	21	1.67	0.28
910-911	29645	0.52	0.09	55.1	2.6	121	17	1.50	0.26
920-911	30604	0.41	0.07	15.6	0.8	139	19	1.14	0.19

69
70

Table S2. RC13-254 trace metal concentrations.

Depth (cm)	Age (yr)	Cd (ppm)	± 1σ (ppm)	Re (ppb)	± 1σ (ppb)	Ag (ppb)	± 1σ (ppb)	Mo (ppm)	± 1σ (ppm)
0-1	3500	0.87	0.15	1.3	0.1	18	3	1.19	0.46
5-6	4625	8.97*	1.56	0.8	0.0	11	2	0.21	0.04
10-11	5750	1.80	0.30	0.2	0.0	14	3	0.38	0.01
15-16	6950	0.13	0.02	0.5	0.0	4	1	0.57	0.01
20-21	8293	3.70*	0.74	0.5	0.0	24	5	0.70	0.14
25-26	9100	0.10	0.02	0.4	0.0	7	1	0.50	0.10
30-31	10100	0.07	0.01	0.6	0.0	1	0	0.91	0.01
35-36	11050	0.08	0.01	0.6	0.0	14	2	0.76	0.01
41-42	11650	0.01	0.00	0.7	0.0	24	3	0.35	0.01
50-51	12393	0.00	0.00	0.8	0.0	20	3	0.28	0.00
61-62	13125	0.02	0.00	1.0	0.0	31	4	0.51	0.01
70-71	13575	0.04	0.01	5.6	0.3	90	13	0.31	0.00
81-82	14179	0.16	0.03	16.6	0.8	153	33	0.30	0.00
90-91	14821	0.38	0.07	24.8	1.1	195	27	0.37	0.01
101-102	15598	1.56	0.25	46.8	2.2	194	42	0.56	0.09
109-110	16120	0.71	0.13	24.6	1.1	193	27	0.78	0.01
125-126	17109	0.31	0.05	19.6	0.9	125	27	0.86	0.14
141-142	17745	0.76	0.13	30.6	1.5	235	53	1.21	0.20
161-162	18109	0.29	0.05	27.1	1.2	118	17	1.12	0.02
171-172	18291	0.48	0.08	21.1	1.0	130	18	1.32	0.21
181-182	19148	0.26	0.05	36.2	1.7	69	15	1.28	0.02
191-192	20041	0.29	0.05	38.5	1.8	79	11	1.44	0.24
205-206	21062	0.43	0.08	25.3	1.2	85	12	1.25	0.02
221-222	21829	0.50	0.10	15.0	0.7	168	24	1.97	0.32
240-241	22913	0.28	0.05	14.2	0.7	116	16	1.50	0.02
261-262	23466	0.35	0.07	16.7	0.8	79	17	1.58	0.03
290-291	24739	0.52	0.09	17.7	0.8	169	24	1.27	0.02
309-310	25440	1.26	0.25	17.3	0.8	204	46	2.92	0.50
330-331	26032	0.71	0.13	7.6	0.4	273	60	1.24	0.21
341-342	26402	0.66	0.12	22.7	1.1	179	25	1.67	0.27
361-362	27768	0.24	0.04	21.4	1.0	241	34	0.74	0.01
371-372	28451	0.22	0.04	12.0	0.6	80	17	0.88	0.14
379-380	28998	0.44	0.08	18.0	0.8	131	29	0.69	0.01

*Indicates suspected contamination.

Table S3. TN057-13-4PC organic carbon concentrations. RSD is 3% based on duplicate analysis of ~10% of samples.

Depth (cm)	Age (yr)	C_{org} (weight %)
0-1	18	2.29*
10-11	305	0.42
20-21	749	0.57
40-41	1259	0.41
60-61	1769	0.27
80-81	2295	0.27
100-101	2824	0.37
120-121	3353	0.29
140-141	3882	0.35
160-161	4410	0.31
180-181	4939	0.31
200-201	5468	0.42
220-221	5997	0.44
240-241	6526	0.49
260-261	6998	0.43
300-301	7549	0.36
340-341	8100	0.41
380-381	8651	0.54
420-421	9203	0.38
470-471	9631	0.36
510-511	10164	0.33
560-561	10988	
580-581	11367	0.31
610-611	11936	0.30
640-641	12505	0.27
670-671	13073	0.37
700-701	13642	0.82*
730-731	14211	0.38
760-761	16163	0.47
770-771	17062	0.42
780-781	17960	0.43
790-791	18859	0.56
800-801	19758	0.60
810-811	20657	0.46
820-821	21556	0.38
830-831	22454	0.37
840-841	23353	0.39
850-851	24252	0.34
860-861	25151	0.35

870-871	26050	0.37
880-881	26949	0.44
890-891	27847	0.48
900-901	28746	0.47
910-911	29645	0.46
920-911	30604	0.38

77 *Indicates suspect measurement

Table S4. RC13-254 organic carbon concentrations. RSD is 3% based on duplicate analysis of ~10% of samples.

Depth (cm)	Age (yr)	C_{org} (weight %)
0-1	3500	1.06
5-6	4625	0.96
10-11	5750	0.66
15-16	6950	0.29
20-21	8293	0.35
25-26	9100	0.30
30-31	10100	0.26
35-36	11050	0.33
41-42	11650	0.36
50-51	12393	0.34
61-62	13125	0.34
70-71	13575	0.36
81-82	14179	0.37
90-91	14821	0.62
101-102	15598	0.62
109-110	16120	0.57
125-126	17109	0.55
141-142	17745	0.82
161-162	18109	0.58
171-172	18291	0.59
181-182	19148	0.57
191-192	20041	0.61
205-206	21062	0.60
221-222	21829	0.66
240-241	22913	0.48
261-262	23466	0.53
290-291	24739	0.66
309-310	25440	0.63
330-331	26032	0.55
341-342	26402	0.54
361-362	27768	0.54
371-372	28451	0.43
379-380	28998	0.59

Table S5. $_{xs}{}^{230}Th_0$ values for RC13-254 (Kumar, 1994).

Depth (cm)	$_{xs}{}^{230}Th_0$ (dpm/g)	$_{xs}{}^{230}Th_0$ 1σ uncertainty (dpm/g)
13	10.34	0.175
18	9.40	0.157
34	7.74	0.167
123	3.06	0.096
172	2.46	0.071
432	4.66	0.151

Supplementary References

Anderson, R. F., Ali, S., Bradtmiller, L. I., Nielsen, S. H. H., Fleisher, M. Q., Anderson, B. E., and Burckle, L. H.: Wind-driven upwelling in the Southern Ocean and the deglacial rise in atmospheric CO_2, Science, 323, 1443-1448, 2009.

Bradtmiller, L. I., Anderson, R. F., Fleisher, M. Q., and Burckle, L. H.: Comparing glacial and Holocene opal fluxes in the Pacific sector of the Southern Ocean. In: Paleoceanography, PA2214, 2009.

Chase, Z., Anderson, R. F., Fleisher, M. Q., and Kubik, P. W.: Accumulation of biogenic and lithogenic material in the Pacific sector of the Southern Ocean during the past 40,000 years, Deep-Sea Research II, 50, 799-832, 2003.

Dezileau, L., Bareille, G., Reyss, J. L., and Lemoine, F.: Evidence for strong sediment redistribution by bottom currents along the southeast Indian ridge, Deep-Sea Research I, 47, 1899-1936, 2000.

Francois, R., Bacon, M. P., Altabet, M. A., and Labeyrie, L. D.: Glacial/interglacial changes in sediment rain rate in the SW Indian sector of Subantarctic waters as recorded by ^{230}Th, ^{231}Pa, U, and δ^{15}N, Paleoceanography, 8, 611-629, 1993.

Francois, R., Frank, M., van der Loeff, M. M. R., and Bacon, M. P.: Th-230 normalization: An essential tool for interpreting sedimentary fluxes during the late Quaternary. In: Paleoceanography, PA1018, 2004.

Kumar, N.: Trace metals and natural radionuclides as tracers of ocean productivity, Ph.D. Ph.D., Columbia University, 336 pp., 1994.

Kumar, N., Anderson, R. F., Mortlock, R. A., Froelich, P. N., Kubik, P., Dittrichhannen, B., and Suter, M.: Increased biological productivity and export production in the glacial Southern Ocean, Nature, 378, 675-680, 1995.

Skinner, L. C., Fallon, S., Waelbroeck, C., Michel, E., and Barker, S.: Ventilation of the deep Southern Ocean and deglacial CO_2 rise, Science, 328, 1147-1151, 2010.

Skinner, L. C., Waelbroeck, C., Scrivner, A. E., and Fallon, S. J.: Radiocarbon evidence for alternating northern and southern sources of ventilation of the deep Atlantic carbon pool during the last deglaciation, Proceedings of the National Academy of Sciences of the United States of America, 111, 5480-5484, 2014.

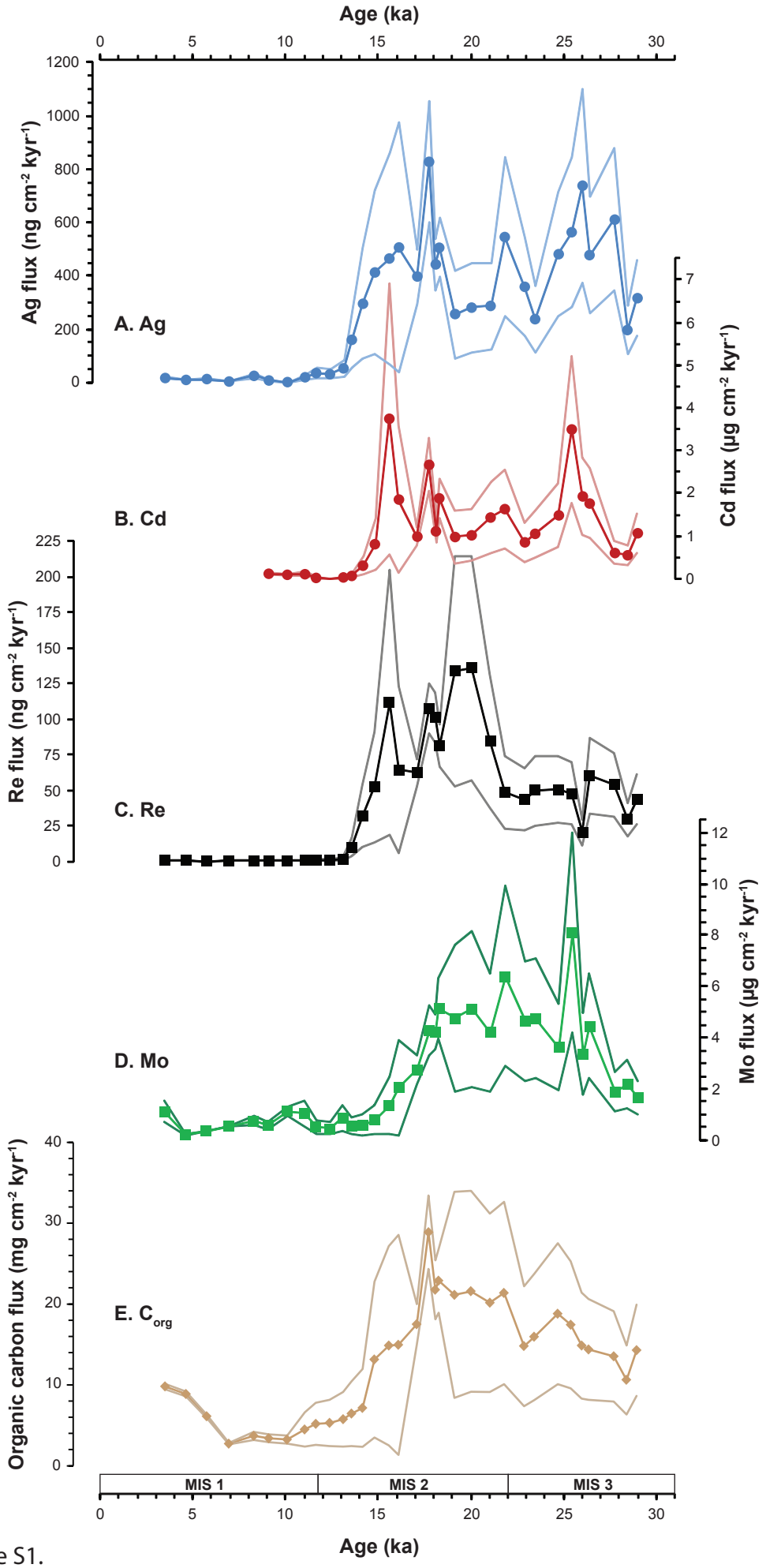
Age (ka)
0
5
10
15
20
25
30
Ag flux (ng cm-2 kyr-1)
1200
1000
800
600
400
200
0
A. Ag
Cd flux (µg cm-2 kyr-1)
7
6
5
4
3
2
1
0
B. Cd
Re flux (ng cm-2 kyr-1)
225
200
175
150
125
100
75
50
25
0
C. Re
Mo flux (µg cm-2 kyr-1)
12
10
8
6
4
2
0
D. Mo
Organic carbon flux (mg cm-2 kyr-1)
40
30
20
10
0
E. Corg
MIS 1
MIS 2
MIS 3
Age (ka)

Figure S1.

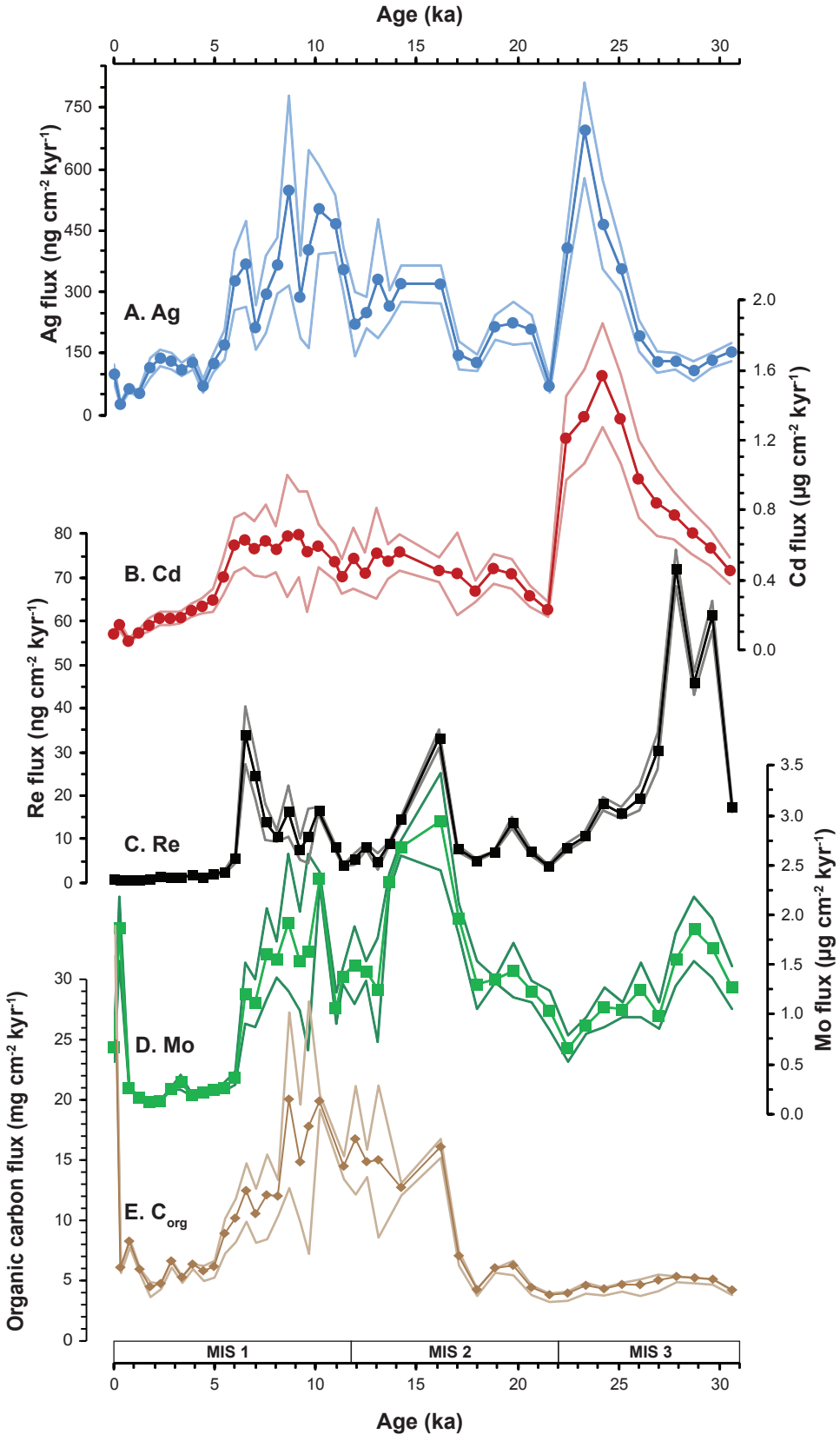
Age (ka)
0
5
10
15
20
25
30
Ag flux (ng cm-2 kyr-1)
750
600
450
300
150
0
A. Ag
Cd flux (µg cm-2 kyr-1)
2.0
1.6
1.2
0.8
0.4
0.0
B. Cd
Re flux (ng cm-2 kyr-1)
80
70
60
50
40
30
20
10
0
C. Re
Mo flux (µg cm-2 kyr-1)
3.5
3.0
2.5
2.0
1.5
1.0
0.5
0.0
D. Mo
Organic carbon flux (mg cm-2 kyr-1)
30
25
20
15
10
5
0
E. Corg
MIS 1
MIS 2
MIS 3
Age (ka)

Figure S2.